

Supporting Information Available

Long lived charge separation in iridium(III) photosensitized polyoxometalates : synthesis, photophysical and computational studies of organometallic-redox tunable oxide assemblies

Benjamin Matt, Xu Xiang, Alexey L. Kaledin, Jamal Moussa, Hani Amouri, Sandra Alves, Craig L. Hill, Tianquan Lian,* Djamaladdin G. Musaev,* Guillaume Izzet, and Anna Proust*

Contents:

1. General Methods
2. Synthesis of complex **2**, **Figure S1**. Enlargement of the 6-9 ppm region of the ^1H NMR spectrum (CD_2Cl_2 , 400 MHz) of complex **2**.
3. Synthesis of **K_{Si}[Ir]**, **Figure S2**. ^1H NMR spectrum of **K_{Si}[Ir]** ($\text{DMSO}-d_6$, 400 MHz)
4. Synthesis of **D_{Si}[Ir]**, **Figure S3**. ^1H NMR spectrum of **D_{Si}[Ir]** ($\text{DMSO}-d_6$, 300 MHz)
5. Synthesis of **D_{Sn}[Ir]**, **Figure S4**. ^1H NMR spectrum of **D_{Sn}[Ir]** (CD_3CN , 300 MHz)
6. **Figure S5**. Transient spectra at indicated delay times (a) and kinetics at indicated wavelengths (b) of complex **2** after 400 nm excitation. The solid line in b) are fits to the data according to a kinetics model described in the main text.
7. Derivation of the kinetics models
8. **Table S0**. Fitting parameters for transient kinetics shown in Figure 3.
9. **Figure S6**. Representative frontier orbitals of **K_{Sn}[Ir]** in DMF.
10. **Figure S7**. Representative frontier orbitals of **K_{Si}[Ir]_{mod}** in DMF.
11. **Figure S8**. Representative frontier orbitals of **D_{Sn}[Ir]** in DMF.
12. **Table S1**: Calculated cartesian coordinates of the **K_{Sn}[Ir]** and **K_{Si}[Ir]_{mod}** (in Å).
13. **Figure S9**. UV-VIS spectra of **K_{Sn}[Ir]** (upper) and **K_{Si}[Ir]_{mod}** (lower) in DMF solution. We constructed these spectra by using the first 50 singlets of **[K_{Sn}[Ir]]** and the first 70 singlets of **K_{Si}[Ir]_{mod}**. The triplet state positions are marked by red sticks.

14. **Table S2.** The first two singlets and triplets and higher lying bright states of $\mathbf{K}_{\text{Sn}}[\text{Ir}]$ and $\mathbf{K}_{\text{Si}}[\text{Ir}]_{\text{mod}}$. The lowest triplet and bright singlet states localized on the [Ir] moiety are marked by one and two asterisks, respectively. Excitation energy in eV/nm, main orbital transition (H stands for HOMO, and L stands for LUMO) and oscillator strength (f) in a.u. are shown.

15. Complete Reference [27j]

Labeling

In the following text, we use the labeling K and D to refer to the Keggin- and Dawson-type anions respectively, and Si and Sn as subscripts to indicate the primary functionalization by two silyl-aryl or one tin-aryl functions. K_{Si} , K_{Sn} , D_{Si} and D_{Sn} thus stand for $[PW_{11}O_{40}\{Si(Aryl)\}_2]^{3-}$, $[PW_{11}O_{39}\{Sn(Aryl)\}]^4-$, $[P_2W_{17}O_{62}\{Si(Aryl)\}_2]^{6-}$ and $[P_2W_{17}O_{61}\{Sn(Aryl)\}]^7-$. Finally, $K_{Si}[Ir]$, $K_{Sn}[Ir]$, $D_{Si}[Ir]$ and $D_{Sn}[Ir]$ refer to the dyads obtained after covalent linking to the cyclometalated iridium.

General Methods.

Solvents including triethylamine and propylamine were dried over suitable reagents and freshly distilled under argon before use. Reagents were obtained from commercial sources and used as received. Reactions were carried out under dry argon by using Schlenk-tube techniques. $[Pd(PPh_3)_2Cl_2]^1$ was synthesized according to literature procedure. Compounds **1**, $K_{Si}[I]$, $D_{Si}[I]$ and $D_{Sn}[I]$ were prepared according to our previously reported synthetic routes.² Microwave assisted syntheses were performed at ambient pressured reactor (Milestone Start S) equipped with a temperature control unit. The 1H (300.13 MHz, 400.13 MHz), and $\{^1H\} ^{31}P$ (121.5 MHz) NMR spectra were obtained at room temperature in 5 mm o.d. tubes on a Bruker Avance II 300 or Bruker Avance III 400) spectrometer equipped with a QNP probehead. IR spectra were recorded from a KBr pellet by using a Biorad FT 165 spectrometer. The ESI mass spectra were recorded by using an LTQ_Oorbitrap hybrid mass spectrometer (Thermofisher Scientific, Bremen, Germany) equipped with an external ESI source operated in the negative ion mode. Spray conditions included a spray voltage of 3 kV, a capillary temperature maintained at 280°C, a capillary voltage of -30 V and a tube lens offset of -90 V. Sample solutions (10 pmol. μL^{-1}) were infused into the ESI source by using a syringe pump at a flow rate of 180 $\mu L.h^{-1}$. UV-visible spectra were recorded on a Jasco V-670 equipped with a ETC-717 Peltier module. Cyclic voltammetry was carried out using an Autolab PGSTAT 100 workstation. A standard three electrode cell was used, which consisted of the working vitrous carbon electrode, an auxiliary platinum electrode, and an aqueous saturated calomel electrode (SCE) equipped with a double junction. The scan rate was 100 mV/s. Spectroelectrochemical studies were conducted with the aid of an optically transparent thin-layer electrochemical cell (OTTEL). The OTTEL consisted of a platinum-mesh working electrode, a platinum-wire counter electrode, and a silver wire reference electrode. Elemental analysis was performed at the Institut des Substances Naturelles, Gif sur Yvette, France.

¹ O. Dangles, F. Guibe, G. Balavoine, S. Lavielle and A. Marquet, *J. Org. Chem.*, 1987, **52**, 4984-4993.

² (a) B. Matt, J. Moussa, L. M. Chamoreau, C. Afonso, A. Proust, H. Amouri and G. Izzet, *Organometallics*, 2012, **31**, 35-38. (b) G. Izzet, M. Ménand, B. Matt, S. Renaudineau, L. M. Chamoreau, M. Sollogoub and A. Proust, *Angew. Chem., Int. Ed.*, 2012, **51**, 487-490. (c) B. Matt, S. Renaudineau, L. M. Chamoreau, C. Afonso, G. Izzet and A. Proust, *J. Org. Chem.*, 2011, **76**, 3107-3112. (d) V. Duffort, R. Thouvenot, C. Afonso, G. Izzet and A. Proust, *Chem. Commun.*, 2009, 6062-6064.

Ultrafast Visible Transient Absorption Measurements. The femtosecond transient absorption spectrometer is based on a regeneratively amplified Ti:sapphire laser system (coherent Legend, 800 nm, 150 fs, 3 mJ/pulse and 1 kHz repetition rate) and the Helios spectrometer (Ultrafast Systems LLC). The excitation pulse at 400 nm was generated by doubling the frequency of the fundamental 800 nm pulse in a β -barium borate (BBO) type I crystal. The energy of the 400 nm pump pulse was controlled to be \sim 250 nJ/pulse with a neutral density filter. The pump beam diameter at the sample was \sim 400 μm , corresponding to an excitation density of \sim 2 $\mu\text{J}/\text{cm}^2$ per pulse. A white light continuum (WLC) (450 \sim 720 nm), used as a probe, was generated by attenuating and focusing 10 μJ of the fundamental 800 nm pulse into a sapphire window. This WLC was split in two parts used as a probe and reference beams. The probe beam was focused with an aluminum parabolic reflector into the sample with a beam diameter of \sim 150 μm . The reference and probe beams were focused into a fiber-coupled multichannel spectrometer with CMOS sensors and detected at a frequency of 1 kHz. To minimize low-frequency laser fluctuations every other pump pulse was blocked with a synchronized chopper (New Focus Model 3501) at 500 Hz, and the absorbance change was calculated with two adjacent probe pulses (pump-blocked and pump-unblocked). The delay between the pump and probe pulses was controlled by a motorized translational stage. Samples were kept in a 1 mm quartz cuvette (NSG Precision Cells) and constantly stirred by a magnetically-coupled stirring system (SYS 114, SPECTROCELL) throughout the measurements. Before measurements, the solution in the cuvette has been degassed and purged with Ar sufficiently and sealed with paraffin films. In all transient absorption spectra, the chirp and time zero correction were performed with Surface Explorer software (v.1.1.5, Ultrafast Systems LCC) using a dispersion correction curve obtained by fitting the representative kinetics of the transient absorption experiments of the solvent. The typical instrument response of our spectrometer is well represented by a Gaussian function with a full width at half-maximum (FWHM) of 180 ± 10 fs.

Measurements at the ns to μs timescales were carried out in an EOS spectrometer (Ultrafast Systems LLC). The pump pulses at 400 nm were generated from the same laser system described above. The probe pulse, a 0.5-ns white-light source operating at 20 kHz, was synchronized with the femtosecond amplifier, and the delay time was controlled by a digital delay generator. The probe light was detected in a fiber-optic-coupled multichannel spectrometer with a complementary metal–oxide–semiconductor (CMOS) sensor. The absorbance change was calculated from the intensities of sequential probe pulses with and without the pump.

Synthesis of Complex 2

A mixture of complex **1** (38.8 mg, 0.06 mmol, 1.1 equiv), 1-iodo-4-(trimethyltin)benzene (0.055 mmol, 1 equiv), $[\text{Pd}(\text{PPh}_3)_2\text{Cl}_2]$ (3 mg, 8 mol %), CuI (1 mg, 8 mol %) in 4 mL of dried and freshly distilled CH₃CN was prepared. After careful degassing with argon for 10 min, freshly distilled Et₃N (1.1 mmol, 20 equiv) was added. The mixture was stirred at 60°C for 60 min under

microwave irradiation. After evaporation of the solvent under vacuo, the residue was dissolved in 30 mL of DCM and washed 3 times with water. The organic phase was then evaporated and precipitated with pentane. The crude was finally purified by column chromatography on alumina gel using first DCM as eluent followed by DCM/MeOH (98/2) to afford **2** as a yellow microcrystalline solid. Yield: 50 %. ^1H NMR (CD_2Cl_2): δ (ppm) 8.70 (ddd, $J = 5.8$ Hz, $J = 1.5$ Hz, $J = 0.7$ Hz, 1H), 8.23 (dd, $J = 8.1$ Hz, $J = 0.7$ Hz, 1H), 8.00 (dd, $J = 8.1$ Hz, $J = 1.9$ Hz, 1H), 7.85–7.96 (m, 3H), 7.73–7.81 (m, 2H), 7.67 (td, $J = 7.7$ Hz, 1.4 Hz, 2H), 7.58 (ddd, $J = 5.8$ Hz, $J = 1.5$ Hz, $J = 0.7$ Hz, 1H), 7.49 (d, $J = 8.1$ Hz, 2H), 7.39 (d, $J = 8.1$ Hz, 2H), 7.17 (ddd, $J = 7.3$ Hz, $J = 5.8$ Hz, $J = 1.4$ Hz, 1H), 7.01 (ddd, $J = 7.3$ Hz, $J = 5.8$ Hz, $J = 1.4$ Hz, 1H), 7.98 (td, $J = 7.5$ Hz, $J = 1.3$ Hz, 1H), 6.93 (td, $J = 7.5$ Hz, $J = 1.3$ Hz, 1H), 6.83 (td, $J = 7.4$ Hz, $J = 1.4$ Hz, 1H), 6.79 (td, $J = 7.4$ Hz, $J = 1.4$ Hz, 1H), 6.39 (ddd, $J = 7.7$ Hz, $J = 1.3$ Hz, $J = 0.5$ Hz, 1H), 6.17 (ddd, $J = 7.7$ Hz, $J = 1.4$ Hz, $J = 0.5$ Hz, 1H), 0.31 (s, $J_{\text{SnH}} = 54.8$ Hz, 9H). IR (KBr, cm^{-1}): ν 3059 (w), 2918 (W), 2220 (w), 1646 (s), 1606 (s), 1583 (s), 1561 (w), 1478 (s), 1438 (w), 1421 (w), 1374 (w), 1334 (m), 1267 (w), 1160 (w), 1062 (w), 1031 (w), 757 (s), 730 (s), 693 (w), 670 (w), 531 (w). Elemental analysis for $\text{C}_{39}\text{SnH}_{32}\text{N}_3\text{IrO}_2$ (%): calcd C 52.89; H 3.64; N 4.74; found C 53.06; H 3.66; N 4.74

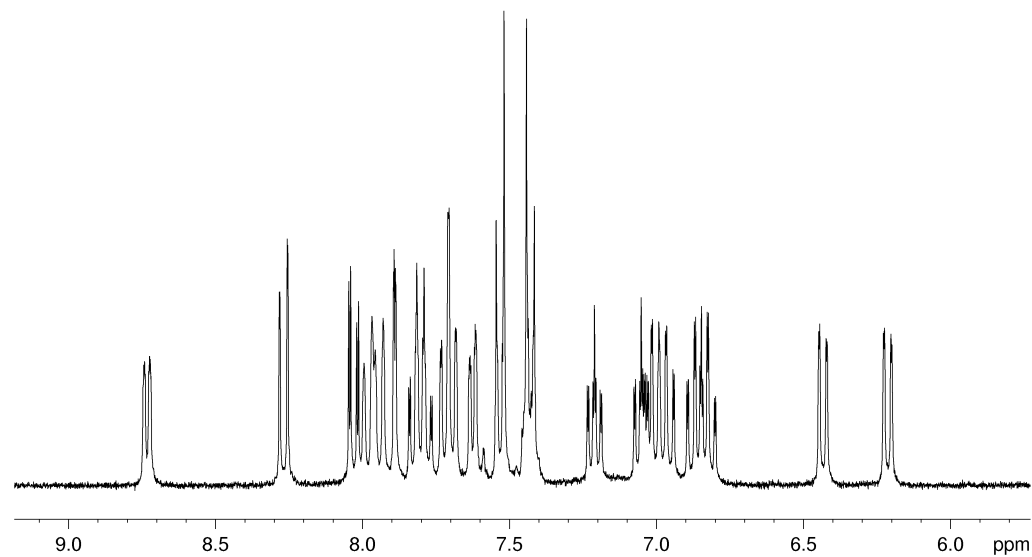


Figure S1. Enlargement of the 6–9 ppm region of the ^1H NMR spectrum (CD_2Cl_2 , 400 MHz) of complex **2**.

Synthesis of $\text{K}_{\text{Si}}[\text{Ir}]$

A mixture of $\text{K}_{\text{Si}}[\text{I}]$ (90 mg, 0.023 mmol, 1 equiv), **1** (45 mg, 0.070 mmol, 3 equiv), $[\text{Pd}(\text{PPh}_3)_2\text{Cl}_2]$ (2.5 mg, 0.0035 mmol, 15 mol %), and CuI (0.7 mg, 0.0035 mmol, 15 mol %), in 5 mL of dried and freshly distilled DMF was prepared. After careful degassing with argon for

10 min, freshly distilled Et₃N (47 mg, 0.46 mmol, 20 equiv) was added. The mixture was stirred at 70°C for 90 min under microwave irradiation. After cooling to room temperature TBABr (20 equiv.) was added and the polyoxometalate was precipitated with Et₂O and triturated in EtOH. The resulting crude was dissolved in DMSO and precipitated with CHCl₃. After filtration and washing with EtOH, **K_{Si}[Ir]** was obtained as a yellow powder. Yield: 79%. ¹H NMR (DMSO-*d*₆): δ (ppm) 8.50 (ddd, J = 5.7 Hz, J = 1.5 Hz, J = 0.7 Hz, 2H), 8.29 (dd, J = 8.1 Hz, J = 1.8 Hz, 2H), 8.21 (m, 4H), 8.09 (d, J = 7.8 Hz, 2H), 7.90-7.97 (m, 4H), 7.86 (dd, J = 7.8 Hz, J = 0.9 Hz, 2H), 7.75-7.80 (m, 8 H), 7.67 (dd, J = 1.8 Hz, J = 0.7 Hz, 2H), 7.47 (d, J = 8.1 Hz, 4H), 7.39 (ddd, J = 7.3 Hz, J = 5.8 Hz, J = 1.4 Hz, 2H), 7.23 (ddd, J = 7.3 Hz, J = 5.8 Hz, J = 1.4 Hz, 2H), 6.96 (ddd, J = 7.3 Hz, J = 5.8 Hz, J = 1.4 Hz, 2H), 6.86 (ddd, J = 7.3 Hz, J = 5.8 Hz, J = 1.4 Hz, 2H), 6.82 (ddd, J = 7.3 Hz, J = 5.8 Hz, J = 1.4 Hz, 2H), 6.72 (ddd, J = 7.3 Hz, J = 5.8 Hz, J = 1.4 Hz, 2H), 6.28 (dd, J = 7.7 Hz, J = 1.0 Hz, 2H), 6.05 (dd, J = 7.7 Hz, J = 1.0 Hz, 2H), 3.17 (m, 24H), 1.57 (m, 24H), 1.32 (sextuplet, J = 7.2 Hz, 24H), 0.94 (t, J = 7.2 Hz, 36H); ³¹P NMR (CD₃CN): δ (ppm) -12.12; MS (ESI): most intense pics, {Aggregates}^{x-} m/z (%): {[POM]}³⁻ 1397.8 (100), calcd 1397.2; IR (KBr, cm⁻¹): ν 3043 (vw), 2961 (s), 2933 (s), 2873 (s), 2220 (vw), 1641 (s) 1606 (s), 1583 (s), 1478 (s), 1378 (w), 1339 (w), 1163 (vw), 1110 (s), 1039 (vs), 966 (vs), 872 (vs), 825 (vs), 760 (s), 524 (m), 384 (s); Elemental analysis for PW₁₁O₄₄Si₂Ir₂C₁₂₀H₁₅₄N₉ (%): calcd C 29.29, H 3.15, N 2.56; found C 28.99, H 3.10, N 2.53.

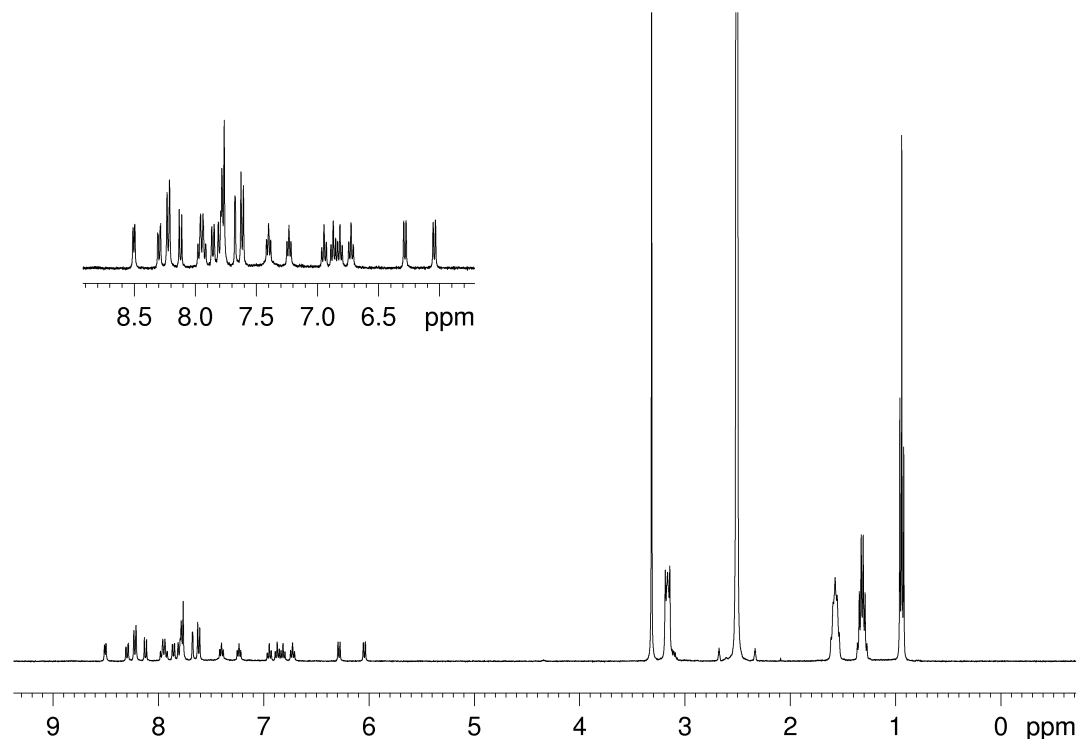


Figure S2. ¹H NMR spectrum of **K_{Si}[Ir]** (DMSO-*d*₆, 400 MHz)

Synthesis of **D_{Si}[Ir]**

A mixture of **D_{Si}[II]** (150 mg, 0.021 mmol, 1 equiv), **1** (48 mg, 0.063 mmol, 3 equiv), [Pd(PPh₃)₂Cl₂] (2.7 mg, 15 mol %), and CuI (0.75 mg, 15 mol %), in 7 mL of dried and freshly distilled DMF was prepared. After careful degassing with argon for 10 min, freshly distilled Et₃N (25 mg, 0.21 mmol, 10 equiv) was added. The mixture was stirred at 70°C for 90 min under microwave irradiation. After cooling to room temperature the polyoxometalate was precipitated with Et₂O. The resulting crude was dissolved in CH₂Cl₂ and after addition of TBABr (20 equiv), the solution was washed 5 times with water. After evaporation of the solvent under reduced pressure, the resulting solid was dissolved in DMSO and precipitated with THF to give **D_{Si}[Ir]** as a yellow powder. Yield: 81%. ¹H NMR (DMSO-d₆): δ (ppm) 8.50 (ddd, J = 5.7 Hz, J = 1.5 Hz, J = 0.7 Hz, 2H), 8.29 (dd, J = 8.1 Hz, J = 1.8 Hz, 2H), 8.21 (m, 4H), 8.09 (d, J = 7.8 Hz, 2H), 7.90-7.97 (m, 4H), 7.86 (dd, J = 7.8 Hz, J = 0.9 Hz, 2H), 7.75-7.80 (m, 8 H), 7.67 (dd, J = 1.8 Hz, J = 0.7 Hz, 2H), 7.47 (d, J = 8.1 Hz, 4H), 7.39 (ddd, J = 7.3 Hz, J = 5.8 Hz, J = 1.4 Hz, 2H), 7.23 (ddd, J = 7.3 Hz, J = 5.8 Hz, J = 1.4 Hz, 2H), 6.96 (ddd, J = 7.3 Hz, J = 5.8 Hz, J = 1.4 Hz, 2H), 6.86 (ddd, J = 7.3 Hz, J = 5.8 Hz, J = 1.4 Hz, 2H), 6.82 (ddd, J = 7.3 Hz, J = 5.8 Hz, J = 1.4 Hz, 2H), 6.72 (ddd, J = 7.3 Hz, J = 5.8 Hz, J = 1.4 Hz, 2H), 6.28 (dd, J = 7.7 Hz, J = 1.0 Hz, 2H), 6.05 (dd, J = 7.7 Hz, J = 1.0 Hz, 2H), 3.17 (m, 48H), 1.57 (m, 48H), 1.32 (sextuplet, J = 7.2 Hz, 48H), 0.94 (t, J = 7.2 Hz, 72H); ³¹P NMR (CD₃CN): δ (ppm) -9.39 et -12.35; MS (ESI): most intense pics, {Aggregates}^{x-} m/z (%): {H[POM]}⁵⁻ 1136.0 (93), calcd 1136.2; {TBA[POM]}⁵⁻ 1184.0 (100), calcd 1184.5; {TBA₂[POM]}⁴⁻ 1540.9 (69), calcd 1541.2; IR (KBr, cm⁻¹): ν 2962 (s), 2933 (s), 2873 (s), 2220 (vw), 1638 (s), 1478 (s), 1379 (w), 1339 (w), 1163 (vw), 1089 (vs), 1040 (m), 954 (vs), 916 (s), 813 (vs), 763 (vs), 531 (m), 390 (s), 329 (m); Elemental analysis for P₂W₁₇O₆₆Si₂Ir₂C₁₆₈H₂₆₂N₁₂ (%): calcd C 28.29, H 3.70, N 2.36; found: C 28.42, H 3.62, N 2.26.

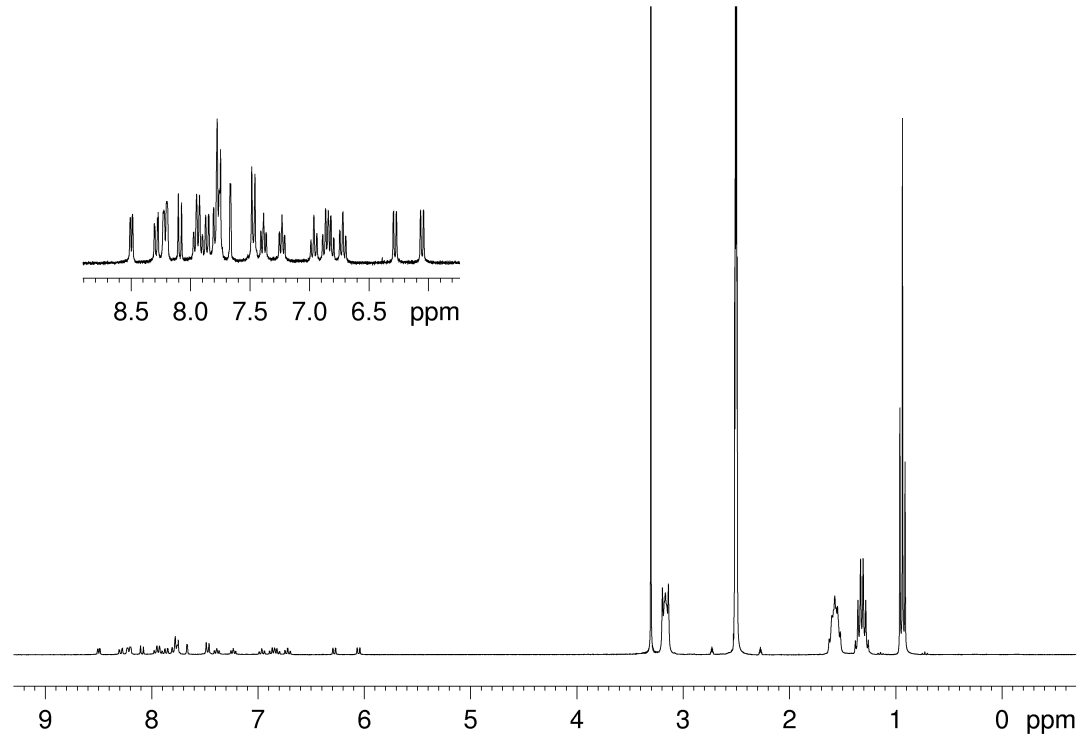


Figure S3. ¹H NMR spectrum of **D_{Sn}[Ir]** (DMSO-*d*₆, 300 MHz)

Synthesis of **D_{Sn}[Ir]**

A mixture of **D_{Sn}[I]** (200 mg, 0.032 mmol, 1 equiv), **1** (37.8 mg, 0.058 mmol, 2 equiv), [Pd(PPh₃)₂Cl₂] (2 mg, 0.0028 mmol, 8 mol %), and CuI (0.5 mg, 0.0028 mmol, 8 mol %), in 5 mL of dried and freshly distilled DMF was prepared. After careful degassing with argon for 10 min, freshly distilled Et₃N (33 mg, 0.32 mmol, 10 equiv) was added. The mixture was stirred at 70°C for 60 min under microwave irradiation. After cooling to room temperature the polyoxometalate was precipitated with Et₂O. The resulting crude was dissolved in CH₂Cl₂ and after addition of TBABr (20 equiv), the solution was washed 5 times with water. After evaporation of the solvent under reduced pressure, the obtained solid was dissolved in CHCl₃ and precipitated with THF. Finally for microanalysis purpose the polyoxometalate was eluted on a Sephadex LH20 column with CH₂Cl₂ to give **D_{Sn}[Ir]** as an orange powder. Yield: 78%. ¹H NMR (CD₃CN): δ (ppm) 8.62 (ddd, J = 5.7 Hz, J = 1.5 Hz, J = 0.7 Hz, 1H), 8.15 (m, 2H), 8.06 (m, 2H), 7.72-7.92 (m, 8H), 7.57 (d + dd, J = 8.1 Hz, J_{SnH} = 32.4 Hz, 2H), 7.29 (ddd, J = 7.3 Hz, J = 5.8 Hz, J = 1.4 Hz, 1H), 7.15 (ddd, J = 7.3 Hz, J = 5.8 Hz, J = 1.4 Hz, 1H), 6.76-7.03 (m, 4H), 6.38 (dd, J = 7.7 Hz, J = 1.0 Hz, 1H), 6.17 (dd, J = 7.7 Hz, J = 1.0 Hz, 1H), 3.17 (m, 56H), 1.66 (m, 56H), 1.43 (sextuplet, J = 7.2 Hz, 56H), 1.00 (t, J = 7.2 Hz, 84H); ³¹P NMR (CD₃CN) :

δ (ppm) -9.54 et -12.46. MS (ESI): most intense pics, {Aggregates}^{x-} m/z (%): {H,TBA[POM]}⁵⁻ 1049.4 (100), calcd 1049.4; {H,TBA₂[POM]}⁴⁻ 1372.1 (75), calcd 1372.3; {H,TBA₃[POM]}³⁻ 1910.9 (40), calcd 1910.6. IR (KBr, cm⁻¹): ν 2961 (s), 2933 (s), 2873 (s), 2220 (vw), 1639 (s), 1480 (s), 1380 (w), 1340 (w), 1163 (vw), 1091 (vs), 950 (vs), 903 (vs), 783 (vs), 525 (m), 385 (s), 368 (s), 331 (m); Elemental analysis for P₂W₁₇O₆₃SnIrC₁₄₈H₂₇₅N₁₀ (%): calcd C 26.53, H 4.14, N 2.09; found C 26.36, H 3.97, N 1.82.

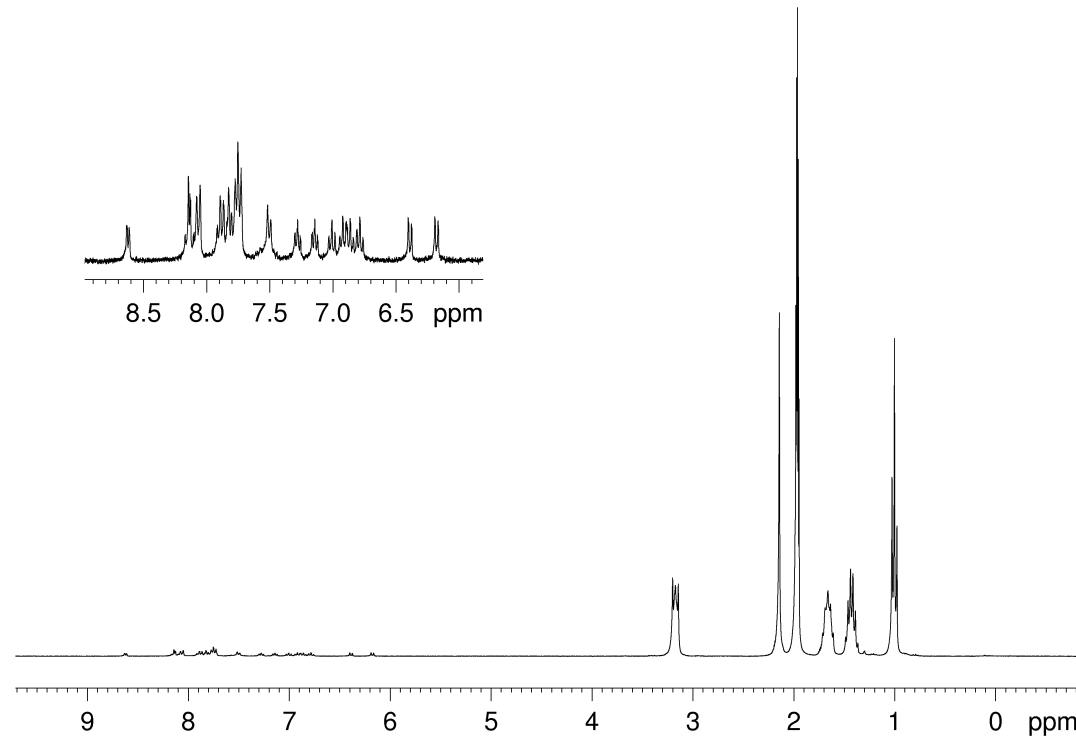


Figure S4. ¹H NMR spectrum of D_{Sn}[Ir] (CD₃CN, 300 MHz)

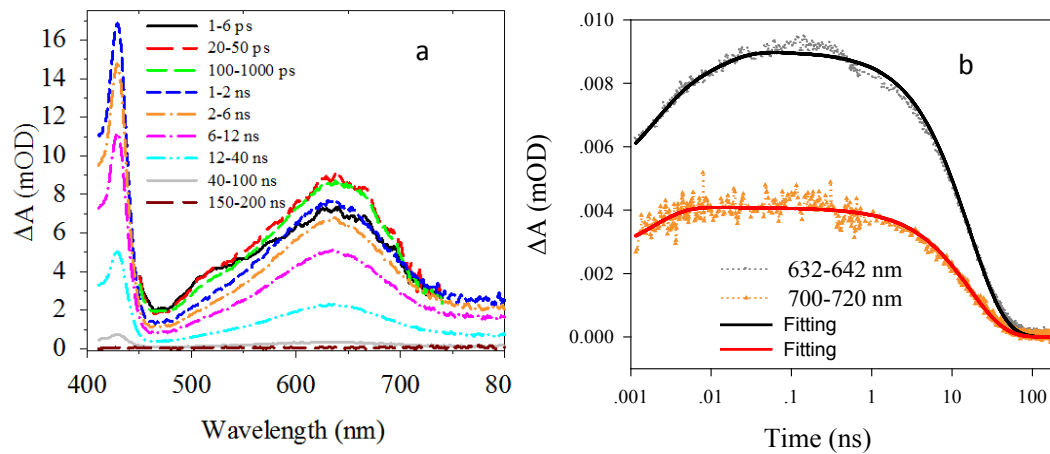


Figure S5. Transient spectra at indicated delay times (a) and kinetics at indicated wavelengths (b) of complex **2** after 400 nm excitation. The solid lines in b) are fits to the data according to a kinetics model described in the main text.

Derivation of the kinetics model.

For complex **2**, we consider two excited states: [Ir*] and [Ir**].

$$\text{The population of } [\text{Ir}^*]: N^*(t) = N_0 \left[a_1 \times e^{-t/t1} + (1-a_1) \times e^{-t/t2} \right];$$

$$\text{The population of } [\text{Ir}^{**}]: N^{**}(t) = N_0 \left\{ -[a_1 \times e^{-t/t1} + (1-a_1) \times e^{-t/t2}] + e^{-t/t3} \right\}$$

The transient absorption signal of 632 nm is given by:

$$\Delta A = \dot{\alpha}_{632}^* \times N^*(t) + \dot{\alpha}_{632}^{**} \times N^{**}(t);$$

$$\Delta A = \dot{\alpha}_{632}^* \times N_0 \left[a_1 \times e^{-t/t1} + (1-a_1) \times e^{-t/t2} \right] + \dot{\alpha}_{632}^{**} \times N_0 \left\{ -[a_1 \times e^{-t/t1} + (1-a_1) \times e^{-t/t2}] + e^{-t/t3} \right\};$$

$$\Delta A = (\dot{\alpha}_{632}^* - \dot{\alpha}_{632}^{**}) \times N_0 \left[a_1 \times e^{-t/t1} + (1-a_1) \times e^{-t/t2} \right] + \dot{\alpha}_{632}^{**} \times N_0 e^{-t/t3};$$

where $\dot{\alpha}_{632}^*$ and $\dot{\alpha}_{632}^{**}$ are extinction coefficients of [Ir*] and [Ir**], respectively, at 632 nm. A similar expression can be derived for the TA signal at other wavelengths. These equations can be described by a general expression used for fitting the kinetics data:

$$\Delta A = -A \times [B \times e^{-\frac{t}{t1}} + (1-B) \times e^{-\frac{t}{t2}}] + C \times e^{-\frac{t}{t3}};$$

For the POM-[Ir] hybrids, in addition to the two excited states (POM-[Ir*] and POM-[Ir**]) that are observed in [Ir] complexes, we also consider a charge separated state (POM-[Ir⁺]). Following the kinetics model shown in scheme 2 in the main text, we can derive the following time-dependent population of these species.

$$\text{The Population of } [\text{Ir}^*]\text{-POM}: N^*(t) = N_0 \left[a_1 \times e^{-t/t1} + (1-a_1) \times e^{-t/t2} \right];$$

$$\text{The population of } [\text{Ir}^{**}]\text{-POM}: N^{**}(t) = N_0 \left\{ -[a_1 \times e^{-t/t1} + (1-a_1) \times e^{-t/t2}] + e^{-(t/t3+t/t4)} \right\};$$

$$\text{The population of the charge separated } [\text{Ir}^+]\text{-POM}: N^+(t) = \frac{1/t3}{1/t3+1/t4} N_0 \left[-e^{-(t/t3+t/t4)} + e^{-t/t5} \right];$$

The TA signal at 632 nm is given by:

$$\Delta A = \dot{\alpha}_{632}^* \times N^*(t) + \dot{\alpha}_{632}^{**} \times N^{**}(t) + \dot{\alpha}_{632}^{+-} \times N^+(t);$$

$$\Delta A = \dot{\alpha}_{632}^* \times N_0 \left[a_1 \times e^{-t/t1} + (1-a_1) \times e^{-t/t2} \right] + \dot{\alpha}_{632}^{**} \times N_0 \left\{ -[a_1 \times e^{-t/t1} + (1-a_1) \times e^{-t/t2}] + e^{-(t/t3+t/t4)} \right\}$$

$$+ \dot{\alpha}_{632}^{+-} \times \frac{1/t3}{1/t3+1/t4} N_0 \left[-e^{-(t/t3+t/t4)} + e^{-t/t5} \right];$$

$$\Delta A = (\dot{\alpha}_{632}^* - \dot{\alpha}_{632}^{**}) \times N_0 \left[a_1 \times e^{-t/t1} + (1-a_1) \times e^{-t/t2} \right] + (\dot{\alpha}_{632}^{**} - \dot{\alpha}_{632}^{+-} \times \frac{1/t3}{1/t3+1/t4}) \times N_0 e^{-(t/t3+t/t4)}$$

$$+ \dot{\alpha}_{632}^{+-} \times \frac{1/t3}{1/t3+1/t4} N_0 e^{-t/t5};$$

The TA signal at 632 nm and other wavelengths can be expressed by the following fitting function: $\Delta A = -A \times [B \times e^{-\frac{t}{t^1}} + (1-B) \times e^{-\frac{t}{t^2}}] + (C-D) \times e^{-(\frac{t}{t^3} + \frac{t}{t^4})} + D \times e^{-\frac{t}{t^5}} + E$; (E for a small long-lived component)

Table S0. Fitting parameters for transient kinetics shown in Figure 3.

Sample	Wavelength (nm)	A	t1 (ns)	B	t2 (ns)	C	t3 (ns)	D	t4 (ns)	t5 (ns)	E
2	637	0.0044	0.0018	0.66	0.011	0.0090	16.8	N/A	N/A	N/A	N/A
	710	0.00097	0.0018	0.66	0.011	0.0041	16.8	N/A	N/A	N/A	N/A
$D_{Sn}[Ir]$	637	0.0017	0.0018	0.66	0.011	0.0041	16.8	0.0007	82	482	0
	710	0.0001	0.0018	0.66	0.011	0.0016	16.8	0.0008	82	482	0
$K_{Sn}[Ir]$	637	0.0021	0.0018	0.66	0.011	0.0058	16.8	0.0010	46.0	177	0.00021
	710	0.0009	0.0018	0.66	0.011	0.0039	16.8	0.0008	46.0	177	0.00021
$D_{Si}[Ir]$	637	0.0010	0.0018	0.66	0.011	0.0062	16.8	0.0036	0.049	26.8	0.00016
	710	0.0023	0.0018	0.66	0.011	0.0042	16.8	0.0046	0.049	26.8	0.00016
$K_{Si}[Ir]$	637	0	0.0018	0.66	0.011	0.0041	16.8	0.0034	0.0039	1.46	0.00006
	710	0.0020	0.0018	0.66	0.011	0.0038	16.8	0.0038	0.0039	1.46	0.0006

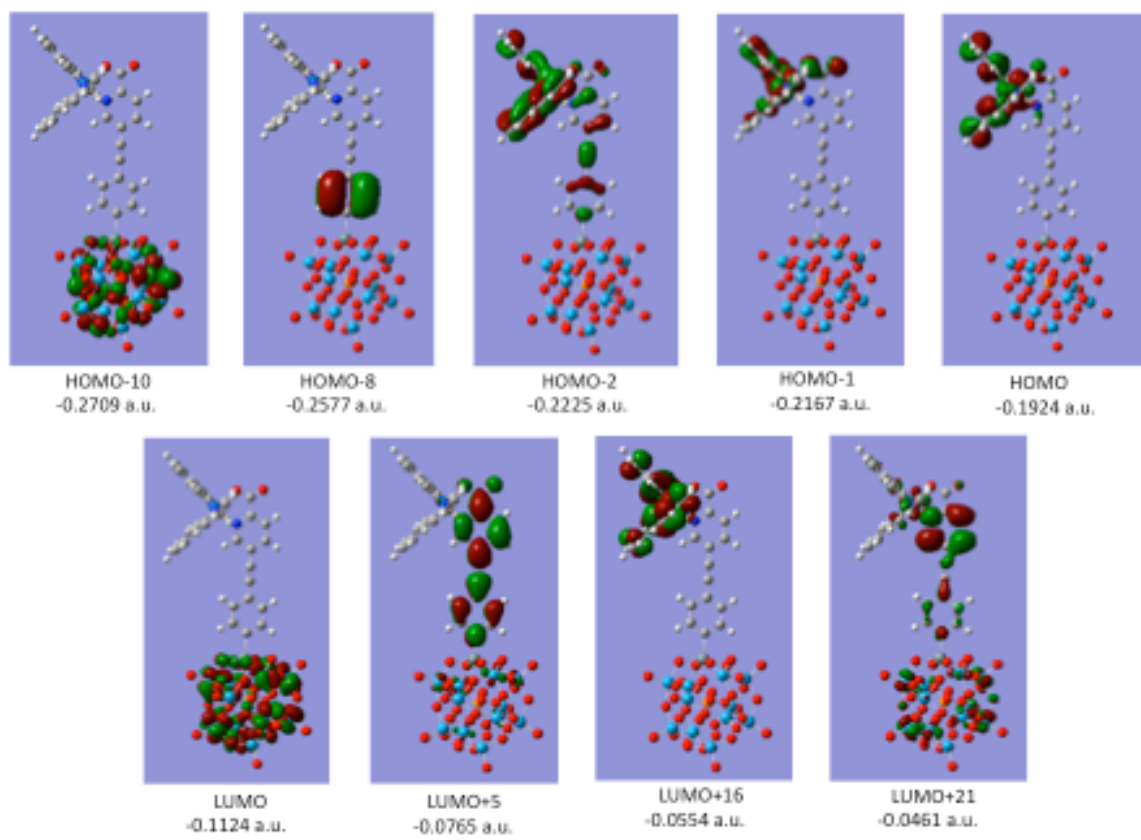


Figure S6. Representative frontier orbitals of $\mathbf{K}_{\text{Sn}}[\text{Ir}]$ in DMF.

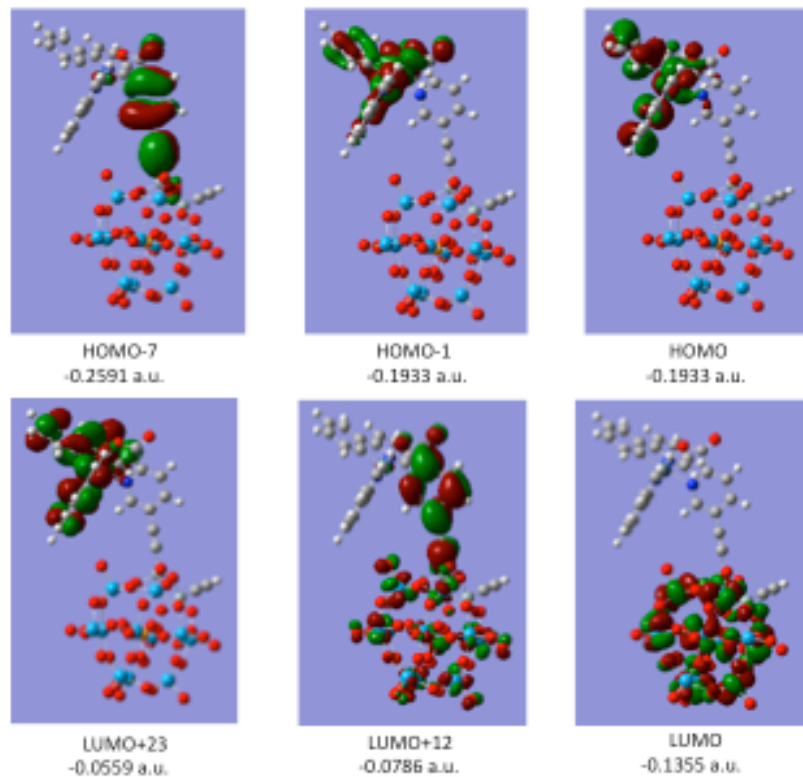


Figure S7. Representative frontier orbitals of $\mathbf{K}_{\text{Si}}[\text{Ir}]_{\text{mod}}$ in DMF.

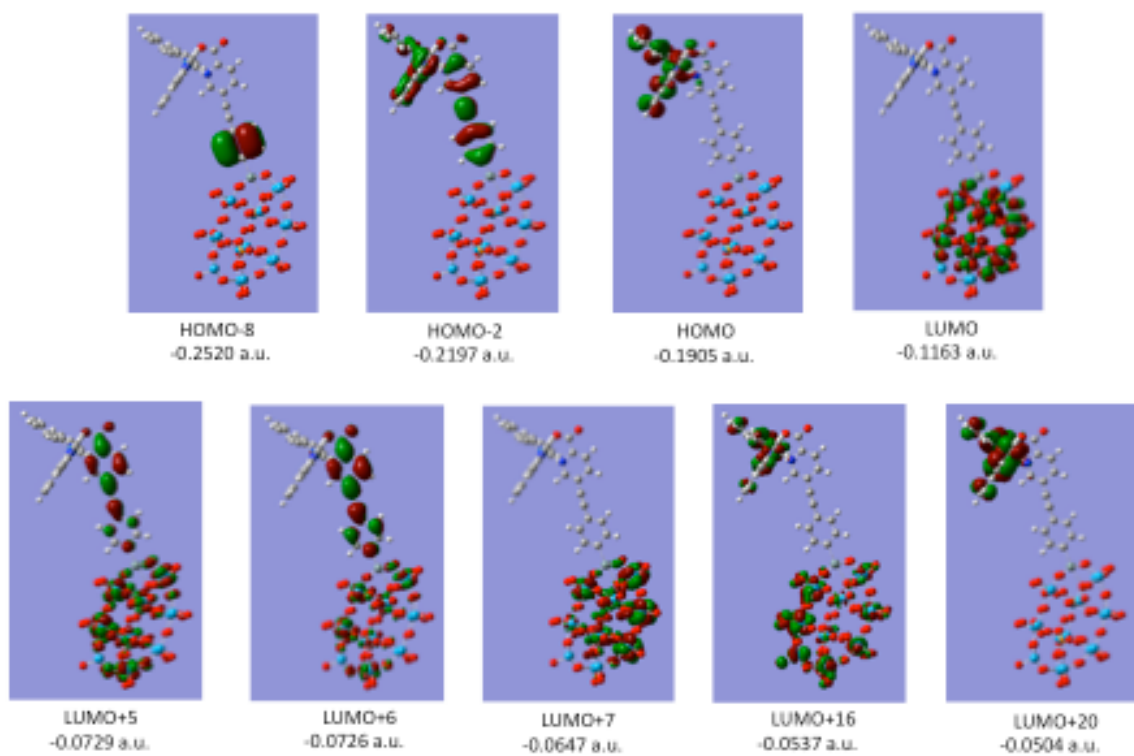


Figure S8. Representative frontier orbitals of $\mathbf{D}_{\mathbf{8n}}[\mathbf{Ir}]$ in DMF.

Table S1. Calculated cartesian coordinates of the **K_{Sn}[Ir]** and **K_{Si}[Ir]_{mod}** (in Å)

K_{Sn}[Ir]								
C	-2.315250	0.784012	0.071128	C	-6.445910	1.657925	0.567263	
C	-3.297017	-0.160356	-0.276206	C	-7.628584	1.903117	0.714133	
C	-2.730458	2.024055	0.586718	C	-9.011764	2.174692	0.888917	
Sn	-0.251970	0.345391	-0.187514	C	-9.974836	1.233162	0.478209	
C	-4.651770	0.120752	-0.117362	N	-11.288672	1.435295	0.630419	
C	-4.081937	2.316864	0.752722	C	-11.730089	2.579447	1.201510	
O	1.949992	-0.344049	-0.760584	C	-9.473955	3.371104	1.471878	
O	-0.015512	0.668413	-2.183714	C	-10.840289	3.565943	1.624035	
O	-0.335461	-1.637786	-0.623159	C	-13.232892	2.744956	1.376430	
O	0.582882	2.143076	0.203451	O	-13.654398	3.804952	1.854804	
O	0.311263	-0.110317	1.705823	O	-13.956866	1.736445	1.021710	
C	-5.061345	1.366218	0.400809	Ir	-12.907901	0.026296	0.082321	
P	3.289279	-0.020805	-0.023185	N	-13.316914	0.859334	-1.774542	
W	1.109439	-2.636166	-1.209253	H	-3.004565	-1.127858	-0.674718	
W	1.491651	0.206197	-3.149272	H	-1.993516	2.773889	0.861097	
W	1.913585	3.119520	1.021746	H	-5.400997	-0.615795	-0.389807	
W	1.513483	0.077264	3.082128	H	-4.390360	3.277897	1.151986	
O	4.490886	-0.677472	-0.756406	H	-9.676913	0.298750	0.016424	
O	3.486649	1.520262	0.010709	H	-8.763316	4.123168	1.796964	
O	3.213525	-0.566161	1.430128	H	-11.245380	4.466586	2.068714	
O	2.997675	-3.036931	-1.584080	H	-12.562444	1.798631	-2.379235	
O	0.370778	-4.119462	-1.650575	C	-12.890245	2.338764	-3.614383	
O	1.118982	-1.667564	-2.882532	C	-14.049947	1.889964	-4.251114	
O	1.664718	-2.953010	0.627856	C	-14.454678	0.404711	-2.384195	
O	3.362345	-0.328572	-3.422246	C	-14.829799	0.921587	-3.632117	
O	0.983656	0.455092	-4.768140	H	-11.674400	2.110988	-1.844795	
O	2.314336	1.911942	-2.683242	H	-12.249160	3.090698	-4.059350	
O	3.753028	3.566377	1.589042	H	-14.340244	2.289069	-5.217651	
O	2.488660	3.797132	-0.716557	C	-15.174114	-0.623032	-1.628495	
O	1.071343	4.473194	1.656858	H	-15.730814	0.559950	-4.112567	
O	1.888510	1.869248	2.490709	C	-14.576883	-0.999829	-0.393705	
O	1.747540	-1.8666714	3.128278	C	-15.230313	-1.992323	0.357444	
O	3.299149	0.106216	3.938191	C	-16.421264	-2.574539	-0.083828	
O	0.519219	0.328544	4.459068	C	-16.372619	-1.209693	-2.069832	
W	5.214255	-0.230814	-3.059302	C	-16.997661	-2.184946	-1.298722	
W	4.831273	-3.074356	-1.131668	H	-14.809772	-2.316721	1.305188	
W	6.878861	-0.505099	-0.035693	H	-16.904081	-3.337959	0.521588	
W	3.711031	2.978598	-1.944453	H	-16.822254	-0.909221	-3.011914	
W	5.370094	2.720607	1.074719	H	-17.923436	-2.638843	-1.639356	
W	4.963843	-0.352122	3.162076	C	-11.758971	-1.486017	-0.578398	
W	2.932603	-2.916820	2.058378	C	-11.344542	-1.756125	-1.894573	
O	5.913181	-0.106182	-4.620908	C	-10.498120	-2.828422	-2.186838	
O	5.245451	-2.140508	-2.774000	C	-10.038683	-3.672834	-1.168616	
O	6.787154	-0.168852	-1.927693	C	-11.285632	-2.359757	0.442673	
O	4.895491	1.604719	-2.595893	C	-10.433812	-3.437120	0.144664	
O	5.298728	-4.676562	-1.527077	H	-11.683789	-1.119597	-2.707012	
O	6.496153	-2.341096	-0.457916	H	-10.193754	-3.008781	-3.214999	
O	4.249951	-3.247250	0.686904	H	-9.380289	-4.504907	-1.398953	
O	8.571804	-0.547236	0.229965	C	-11.745652	-2.047281	1.798048	
O	6.167873	-0.800899	1.712896	H	-10.075305	-4.092827	0.933069	
O	6.446853	1.335361	0.262684	N	-12.555682	-0.948533	1.873080	
O	3.896460	4.212037	-3.120365	C	-13.060609	-0.554142	3.058345	
O	5.107717	3.450836	-0.684411	C	-12.786109	-1.229335	4.239083	
O	6.556978	3.778736	1.715771	C	-11.436968	-2.760172	2.964982	
O	5.138497	1.445088	2.498709	C	-11.956132	-2.352917	4.187797	
O	6.011809	-0.352612	4.518848	H	-13.694384	0.324123	3.024962	
O	4.369534	-2.181835	3.129226	H	-13.213886	-0.879470	5.171373	
O	2.748271	-4.469023	2.761718	H	-10.794046	-3.630252	2.908354	
				H	-11.718182	-2.904719	5.091517	

K_{Si}[Ir] mod								
O	2.168156	1.641522	-0.081716	C	-7.635190	2.055095	3.560480	
O	1.589033	3.998252	1.335797	C	-8.433937	1.419437	2.611393	
O	0.796529	3.801504	-1.235040	C	-6.615026	1.129928	1.190624	
O	-0.481711	1.328531	2.154240	N	-7.919662	0.972692	1.443013	
O	-1.232997	1.140376	-0.399986	H	-5.635497	2.715296	4.036646	
P	2.324651	0.108993	-0.015112	H	-8.100479	2.397271	4.476553	
W	2.372779	3.031528	-2.041696	C	-9.921171	1.193793	2.856581	
W	3.378556	3.281338	1.211166	H	-6.253774	0.752991	0.240704	
W	-0.119626	-0.480166	2.737167	Ir	-9.400112	-0.013828	0.124611	
W	-1.202895	-0.742226	-0.836629	O	-10.550999	0.545244	1.935843	
O	3.789107	-0.285606	-0.432191	O	-10.411319	1.624587	3.906758	
O	2.056374	-0.441660	1.421165	N	-10.085502	1.729212	-0.776514	
O	1.326763	-0.620093	-0.969799	N	-8.777157	-1.831731	0.894151	
O	3.928126	1.949444	-2.355431	C	-9.214528	-2.347122	2.059956	
O	2.563146	4.134937	-3.334328	C	-8.759481	-3.564925	2.545247	
O	3.361031	3.881873	-0.618152	C	-7.814313	-4.271172	1.795861	
O	1.368740	1.606402	-2.834090	C	-7.857263	-2.507703	0.141664	
O	4.882081	2.180263	0.753970	C	-7.364037	-3.739768	0.593552	
O	4.217020	4.541333	2.007224	H	-9.943576	-1.746937	2.591519	
O	3.042351	2.020519	2.619513	H	-9.137941	-3.944352	3.487301	
O	0.678117	-2.217862	2.850339	H	-7.433833	-5.225435	2.146147	
O	1.326477	0.196040	3.792491	C	-7.486667	-1.828035	-1.102241	
O	-1.387723	-0.693339	3.860063	H	-6.631853	-4.274782	0.000817	
O	-0.888624	-1.000964	1.051584	C	-8.140696	-0.584096	-1.335198	
O	-0.624238	-0.285415	-2.597512	C	-7.807271	0.103652	-2.515465	
O	-0.540869	-2.516395	-1.127990	C	-6.873256	-0.409019	-3.419272	
O	-2.872963	-1.039994	-1.019403	C	-6.550531	-2.342955	-2.015199	
W	5.809185	0.518040	0.692573	C	-6.242970	-1.635623	-3.174397	
W	4.809807	0.278989	-2.587698	H	-8.280585	1.056428	-2.734931	
W	4.828865	-2.519840	-0.589187	H	-6.637363	0.147062	-4.323418	
W	3.226216	0.253343	3.367230	H	-6.061306	-3.294723	-1.828537	
W	2.348047	-2.858538	2.152892	H	-5.524607	-2.036395	-3.883227	
W	1.258006	-3.131770	-1.392241	C	-9.515536	2.943187	-0.638627	
W	1.191159	-0.256882	-3.311412	C	-10.033174	4.084018	-1.234815	
O	7.350241	0.931443	1.305858	C	-11.192276	3.965466	-2.005297	
O	6.055394	0.769938	-1.205863	C	-11.218164	1.592296	-1.532123	
O	6.041556	-1.364280	0.350084	C	-11.781759	2.716433	-2.151807	
O	4.803241	0.108387	2.283668	H	-8.618911	2.983289	-0.033532	
O	5.730195	0.540105	-4.004222	H	-9.535938	5.036584	-1.094196	
O	5.259537	-1.555298	-2.191066	H	-11.628532	4.835297	-2.485750	
O	3.103465	-0.303527	-3.281912	C	-11.725866	0.221000	-1.614834	
O	5.763914	-3.939069	-0.766160	H	-12.679839	2.605436	-2.747035	
O	3.163971	-3.009683	-1.405782	C	-10.967601	-0.752439	-0.907013	
O	3.925951	-2.812918	1.079576	C	-11.411945	-2.084376	-0.975089	
O	3.877188	0.597844	4.909608	C	-12.556043	-2.435797	-1.696063	
O	3.177553	-1.677633	3.420799	C	-12.876698	-0.134908	-2.339209	
O	2.478331	-4.378178	2.921536	C	-13.293736	-1.462080	-2.379989	
O	1.436474	-3.264890	0.511303	H	-10.861414	-2.863973	-0.456366	
O	0.998165	-4.746722	-1.883312	H	-12.874868	-3.475061	-1.727608	
O	1.196601	-2.169673	-3.057582	H	-13.450028	0.617997	-2.872689	
O	0.855891	-0.158658	-4.984464	H	-14.182518	-1.737345	-2.939978	
Si	0.370608	4.319470	0.271747					
Si	-1.433306	1.999979	0.990587					
C	0.038257	6.103975	0.238179					
C	-3.179985	1.964969	1.490598					
O	-1.011079	3.568501	0.754481					
C	-0.175134	7.299543	0.210981					
C	-4.361493	1.877216	1.779774					
C	-5.743837	1.753150	2.101213					
H	-0.364618	8.351210	0.188437					
C	-6.279086	2.227301	3.312891					

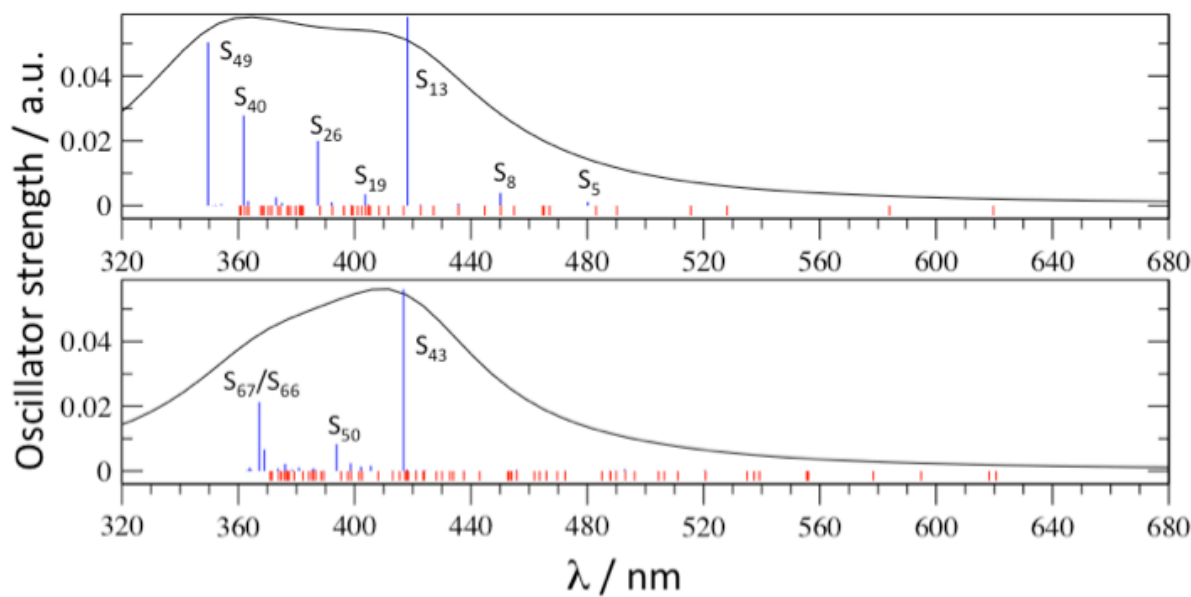


Figure S9. Calculated UV-VIS spectra of $K_{Sn}[Ir]$ (upper) and $K_{Si}[Ir]_{mod}$ (lower). We constructed these spectra by using the first 50 singlets of $[K_{Sn}[Ir]$ and the first 70 singlets of $K_{Si}[Ir]_{mod}$. The triplet state positions are marked by red sticks.

Table S2. The first two singlets and triplets and higher lying bright states of $K_{Sn}[Ir]$ and $K_{Si}[Ir]_{mod}$. The lowest triplet and bright singlet states localized on the [Ir] moiety are marked by one and two asterisks, respectively. Excitation energy in eV/nm, main orbital transition (H stands for HOMO, and L stands for LUMO) and oscillator strength (f) in a.u. are shown.

$K_{Sn}[Ir]$	$K_{Si}[Ir]_{mod}$
S_2/T_2 : 2.12/584 H->L+1 f=0.0	S_2/T_2 : 1.40/883 H -> L+1 f=0.0
* T_5 : 2.53/490 H->L+5 f=0.0	* T_{27} : 2.50/496 H->L+12 f=0.0
** S_{13} : 2.96/418 H->L+16 f=0.0582	** S_{43} : 2.97/417 H->L+23 f=0.0560
S_{19} : 3.07/403 H->L+19 f=0.0035	S_{50} : 3.15/394 H-1->L+12 f=0.0083
S_{26} : 3.20/387 H-1->L+5 f=0.0200	S_{66} : 3.36/367 H-2->L+6 f=0.0067
S_{40} : 3.43/362 H-2->L+5 f=0.0278	S_{67} : 3.37/367 H-2->L+6/12 f=0.0212
S_{49} : 3.55/350 H-3->L+5 f=0.0504	

Complete Reference [27j]

Gaussian 09, Revision A.2, Frisch, M. J.; Trucks, G. W.; Schlegel, H. B.; Scuseria, G. E.; Robb, M. A.; Cheeseman, J. R.; Scalmani, G.; Barone, V.; Mennucci, B.; Petersson, G. A.; Nakatsuji, H.; Caricato, M.; Li, X.; Hratchian, H. P.; Izmaylov, A. F.; Bloino, J.; Zheng, G.; Sonnenberg, J. L.; Hada, M.; Ehara, M.; Toyota, K.; Fukuda, R.; Hasegawa, J.; Ishida, M.; Nakajima, T.; Honda, Y.; Kitao, O.; Nakai, H.; Vreven, T.; Montgomery, Jr., J. A.; Peralta, J. E.; Ogliaro, F.; Bearpark, M.; Heyd, J. J.; Brothers, E.; Kudin, K. N.; Staroverov, V. N.; Kobayashi, R.; Normand, J.; Raghavachari, K.; Rendell, A.; Burant, J. C.; Iyengar, S. S.; Tomasi, J.; Cossi, M.; Rega, N.; Millam, N. J.; Klene, M.; Knox, J. E.; Cross, J. B.; Bakken, V.; Adamo, C.; Jaramillo, J.; Gomperts, R.; Stratmann, R. E.; Yazyev, O.; Austin, A. J.; Cammi, R.; Pomelli, C.; Ochterski, J. W.; Martin, R. L.; Morokuma, K.; Zakrzewski, V. G.; Voth, G. A.; Salvador, P.; Dannenberg, J. J.; Dapprich, S.; Daniels, A. D.; Farkas, Ö.; Foresman, J. B.; Ortiz, J. V.; Cioslowski, J.; Fox, D. J. Gaussian, Inc., Wallingford CT, **2009**